

DAMAGE PROCESS IN AL-ALLOY SPECIMENS: XRDD EXPERIMENT AND NUMERICAL SIMULATION

J. Korouš¹, D. Vavřík^{1,2}, J. Jakůbek², S. Pospíšil²

¹ ITAM CAS, Prosecká 76, 190 00 Prague 9, Czech Republic, korous@itam.cas.cz, vavrik@itam.cas.cz

² IEAP CTU, Horská 3a/22, 128 00 Prague 2, Czech Republic

Abstract

This paper deals with experimental observation of material damage evolution in flat specimens made of aluminium alloy and numerical simulation of this process. The “X-ray Dynamic Defectoscopy” was used for the damage detection. This method makes possible to detect the thickness reduction due to voids evolution and contraction of the specimen. Moreover, surface strain was measured by “Optical Method of Interpolated Ellipses”. The simulation of the specimen behaviour was performed by application of finite element method in which the Gurson-Tvergaard-Needleman plasticity model had been implemented. The critical volume fraction f_c , at which coalescence starts, was determined using Thomason’s limit load solution. The calculated damage was compared with the experimentally determined values.

Introduction

For many metallic materials, ductile fracture is typical. This phenomenon is strictly influenced by presence of voids. The void evolution has typically three stages: nucleation, growth and coalescence. The process can be described using so-called micromechanical models. At present, there are several such models. A well-known plasticity model for porous materials was proposed by Gurson [1]. The model is based on the assumption that a spherical void is surrounded by an incompressible matrix material. Tvergaard and Needleman [2] developed this model later in order to describe the coalescence of voids and improve the prediction of failure. They introduced a modified void volume fraction which simulates the acceleration of voids growth after the coalescence.

The disadvantage of the Gurson-Tvergaard-Needleman model (GTN model) is that it contains many constants which must be determined experimentally. Experiments do not provide the constants directly but they are usually followed by a numerical simulation which fits the investigated parameters.

The objective of this paper is to compare numerical simulations with the experiment where an advanced method based on X-ray detection is used. The comparison was made in order to identify some parameters of the GTN model.

Experiment

The experimental observation of material damage evolution was performed on specimens made of aluminium alloy. The geometry of the specimens is showed in fig. 1.

A new experimental method called “X Ray Dynamic Defectoscopy (XRDD)” was developed for the above mentioned purpose. The experimental equipment and the procedure used was described in detail in the paper published by Vavřík *et al.* [3]

During the loading process, the test specimen was illuminated by X-ray and a position sensitive semiconductor single photon counting pixel detector was used for transmission changes measurement. The detected changes in transmission represented alterations of effective thickness of the specimen. The effective thickness changes were understood as weakening of the material due to void volume fraction and transversal thickness reduction (contraction) resulting from loading stress. Alterations in the specimen thickness due to void volume fraction were separated from the total thickness reduction by deconvolution through Fourier transformation.

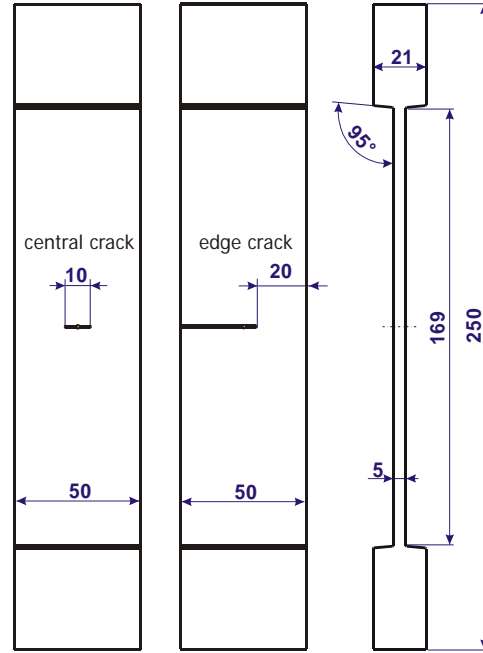


FIGURE 1. Geometry of the specimen used in experiment.

The specimens were loaded in the specially designed loading frame. As the loading was displacement controlled, the axial force was measured by a special load gauge. A strain gauge was cemented on the side of the specimen to measure the axial strain.

We observed step by step the damage zone shape and the proportional volume fraction of voids (damage intensity) by XRDD. Results obtained by XRDD provided a nice visualization of performed physical processes and their correlations with other quantities such as surface strain evolution which is measured using the “Optical Method of Interpolated Ellipses” [3]. Principal strain evolution yields knowledge of evolution of plastic strain field by numerical post processing.

Plasticity model

For the numerical simulation, the above mentioned GTN model was applied. In this case, the plasticity criterion is given by equation [1]:

$$\left(\frac{q}{\bar{\sigma}}\right)^2 + 2q_1 f^* \cosh\left(q_2 \frac{3\sigma_m}{2\bar{\sigma}}\right) - (q_1 f^*)^2 - 1 = 0, \quad (1)$$

where q is the von Mises equivalent stress, σ_m is the mean stress, $\bar{\sigma}$ is the flow stress of the matrix material, q_1 and q_2 are material parameters and f^* is the modified void volume fraction defined by equations [2]:

$$\begin{aligned}
f^* &= f && \text{for } f \leq f_c \\
f^* &= f_c + \frac{1/q_1 - f_c}{f_F - f_c} (f - f_c) && \text{for } f > f_c,
\end{aligned} \tag{2}$$

In Eq. (2), the parameter f_c is the void volume fraction at which coalescence starts and f_F is the void fraction corresponding to the final fracture. Originally, the volume fracture f_c was assumed as a constant but this assumption increased the number of unknown material parameters. That is why, the volume fracture f_c was calculated using the equation proposed by Zhang [4] which was based on the limit load analysis of a cell containing a void. This analysis was performed by Thomason [5]. The coalescence starts when the following condition is satisfied [4]:

$$\frac{\sigma_1}{\bar{\sigma}} = \left[0.1 \left(\frac{1}{\tilde{r}} - 1 \right)^2 + \frac{1.2}{\sqrt{\tilde{r}}} \right] (1 - \pi \tilde{r}^2). \tag{3}$$

The parameter \tilde{r} is calculated from the current volume fraction f and the principal strains ε_1 , ε_2 and ε_3 according equation [4]:

$$\tilde{r} = \frac{\sqrt[3]{0.75 f \exp(\varepsilon_1 + \varepsilon_2 + \varepsilon_3) / \pi}}{0.5 \sqrt{\exp(\varepsilon_2 + \varepsilon_3)}}. \tag{4}$$

The volume fraction f represents an internal state variable. An infinitesimal increase in f can be described according Chu and Neeldeman [6] in the following manner:

$$df = (1 - f) d\varepsilon_{kk} + A d\varepsilon^p \tag{5}$$

The first part on the right side of Eq. (5) represents the growth of existing voids whereas the second part represents the nucleation of new voids. For the nucleation intensity parameter A , Chu and Needleman [6] proposed a statistical description:

$$A = \frac{f_N}{s_N \sqrt{2\pi}} \exp \left[-\frac{1}{2} \left(\frac{\bar{\varepsilon}^p - \varepsilon_N}{s_N} \right)^2 \right], \tag{6}$$

where f_N is the volume fraction of void nucleating particles, ε_N is the mean strain for nucleation, s_N is corresponding standard deviation and $\bar{\varepsilon}^p$ is the equivalent plastic strain.

All FEM simulations were performed by the research code WARP3D [7]. Fig. 2 shows the finite element mesh used for the specimen with a central crack. Due to the symmetry, a quarter of the specimen was modelled only. Similarly to the experiment, the FEM analysis was displacement controlled and the displacements were prescribed on the top surface of the specimen FEM model. The axial force was given as the sum of all nodal reactions in the axial direction in the nodes where the non-zero displacement was prescribed.

The parameters were q_1 and q_2 estimated from Young's modulus and yield stress using the results published by Faleskog *et al.* [8] and the values $q_1 = 1.6$ and $q_2 = 0.88$ were used. The void fraction f_c was calculated using the criterion (3) which was checked after each convergent load step. The constants in eq. (6) was estimated as $f_N = 0.01$, $\varepsilon_N = 0.08$ and $s_N = 0.005$. These values were based on experimental XRDD observations, which indicated a rapid damage growth for the local strain value about 0.08. It should be noted that this value was a rough estimate which needs revision in future. The void volume fraction at final fracture f_F was a free parameter which was determined by fitting of FEM simulations on the experimental results. After reaching the critical void volume, the element was deleted from

the model using the extinction technique. This method is available in the code WARP3D and allows simulating the crack growth.

As the XRDD detected the thickness reduction, the calculated void volume fraction had to be recalculated to obtain a similar damage measure. A simple method was applied. The averaged void volume fraction in each element was determined and from this value the volume V_v of a spherical void was calculated. It was assumed that there is only one void of the volume V_v in each element. The diameter of this void represented local thickness reduction. The relative thickness reduction due to voids was given as sum of the spherical voids diameters divided by the current calculated thickness of the specimen.

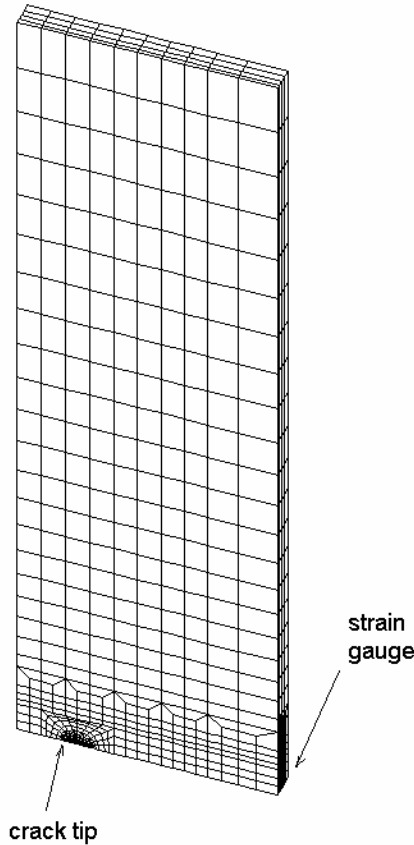


FIGURE 2. FEM mesh of specimen.

Results

Several numerical simulations were performed for different values of the initial void volume fraction f_0 and void volume fraction f_F . The FEM calculations were discontinued near the point of the maximal measured axial force.

Fig. 3 shows the dependence of the calculated and measured axial force on the axial strain for the case when $f_0 = 0.005$. This choice of the initial void volume fraction f_0 led to the best fit of numerical results on the measured values. The calculated axial strain was evaluated in the point where the strain gauge was placed. This point is indicated in Fig. 2. As follows from the Fig. 2, the calculated and measured values of the axial force are very similar. The change of the void volume fraction f_F from 0.12 to 0.15 did not affect the results significantly. However, better fit was reached for $f_F = 0.12$.

The calculated value of f_c using the criterion (3) was about 0.02. This value was not significantly affected by changing others parameters of the model.

The graph in Fig. 3 compares the detected and calculated relative thickness reduction due to damage ahead the crack tip. The plotted dependencies correspond to the loading when the measured force reached its maximum. It should be noted that an assumption was made in order to compare the measured and calculated values. During the experiment, The XRDD did not detect the thickness reduction higher then 0.3. However, the simulation of the crack growth by element extinction assumed that the damage of the deleted elements equals 1. Provided the observed and the simulated processes were the same (i.e. crack growth) the relative thickness reduction was assumed 0.3 in the deleted elements.

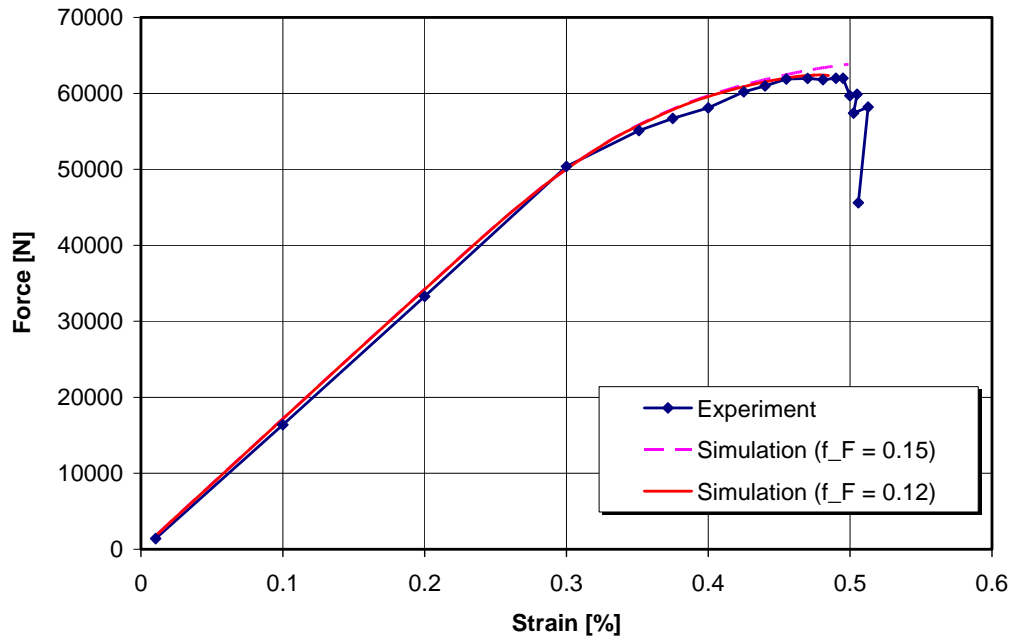


FIGURE 3 Measured and calculated axial force vs. axial strain for $f_0 = 0.005$.

The different values of the void volume fraction f_f influenced the calculated values strongly. Better fit was reached in the case when $f_f = 0.12$.

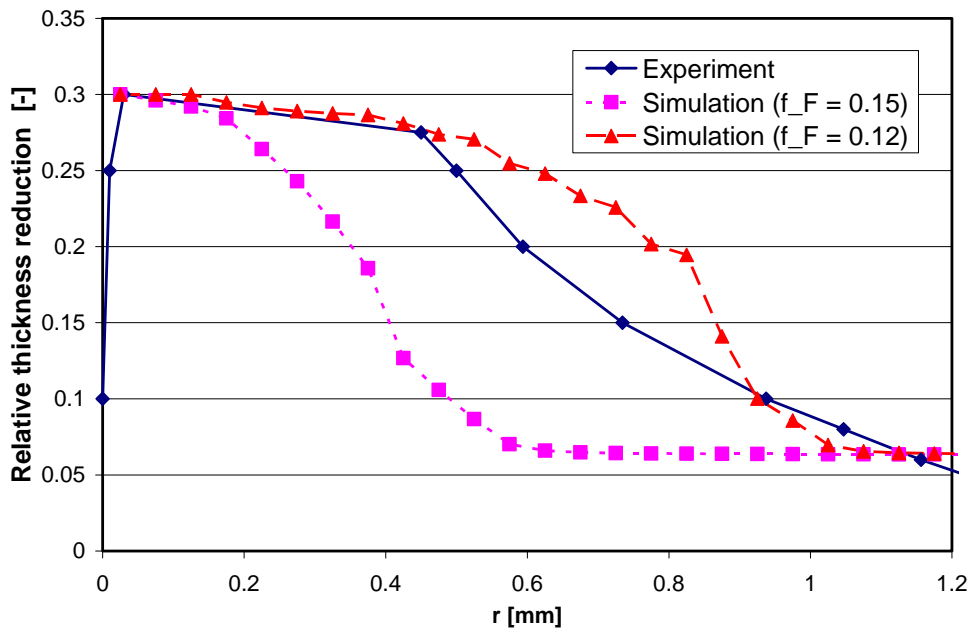


FIGURE 4 Relative thickness reduction ahead the crack tip for $f_0 = 0.005$.

Conclusions

Flat specimens were investigated using “X Ray Dynamic Defectoscopy (XRDD)” and several numerical simulations were performed in order to identify some material parameters of the GTN plasticity model. The results of numerical simulations were compared with the experimental measurement performed by XRDD. The calculated dependence of the axial force on the axial strain agreed well with the measured data. The calculated relative thickness reduction of the specimen differed from the measured values in dependence on the volume fraction f_F . Quite satisfactory results were obtained for $f_F = 0.12$.

Although the results indicated some way how to identify parameters of the GTN model, there are some problems to be solved in future. For example, the influence of the mesh density ahead the crack tip must be investigated and the method how to compare the detected and calculated relative thickness reduction have to be verified better. Also the constants related to the void nucleation should be specified with higher precision.

The “X Ray Dynamic Defectoscopy (XRDD)” promises unique possibilities of damage detection. With connection to numerical simulations, the method can be beneficial in the parameter identification of the micromechanical models such as the GTN plasticity model.

Acknowledgement

The experimental work was carried out within the framework of the Medipix Collaboration based at CERN (see: www.cern.ch/medipix). This work was made possible by the Grant No. 101/03/0731 from the Grant Agency of the Czech Republic. This work was also partly supported by the Ministry of Education, Youth and Sports of the Czech Republic under Research Program MSM 210000018 and by the Czech Committee for Collaboration with CERN under a grant of Ministry of Industry and Trade of the Czech Republic.

References

1. Gurson, A.L., *J. Engng. Mater. Techn.*, vol. **99**, 2-15, 1977.
2. Tvergaard, V. and Needleman, A., *Acta Metall.*, **32**, 157-169, 1984
3. Vavřík, D., Jakubek, J., Visshers, J., Pospíšil, S., Zemánková, J., In *Proceedings of the 14th Biennial Conference on Fracture ECF 14*, edited by A. Neimitz, I.V. Rokach, D. Kocanda, K. Golos, 485-493.
4. Zhang Z.L., In *Nonlinear Fracture and Damage Mechanics*, edited by M.H. Aliabadi, WIT Press, Southampton, 2001, 223-248.
5. Thomason, P.F., *Ductile Fracture of Metals*, Pergamon Press, Oxford, 1990
6. Chu C.C., Needleman A. *J. Engng. Mater. Techn.*, vol. **102**, 249-256, 1980.
7. Gullerud, A.S., Koppenhoefer, K.C., Roy, A., Doods, R.H. Jr., *WARP3D: 3-D Dynamic Nonlinear Fracture Analysis of Solids Using Parallel Computers and Workstations*, Structural Research Series (SRS) 607, UILU-ENG-95-2012, University of Illinois at Urbana-Champaign, 2000
8. Faleskog, J., Gao, X. and Shih, C.F., *Int. J. Fract.*, vol. **89**, 355-373, 1998.